SIMPLIFICATION OF SPATIAL STRUCTURES BY SIMULATION WITH PERIODIC BOUNDARIES

A. Nentchev, R. Sabelka, and S. Selberherr

Institute for Microelectronics, TU Vienna, Gußhausstraße 27–29, A-1040 Wien, Austria
Phone: +43-1-58801/36028, Fax: +43-1-58801/36099, Email: nentchev@iue.tuwien.ac.at

Abstract

This article treats the implementation of periodic boundary conditions for electrical field calculation and capacitance extraction in the simulation software *Smart Analysis Programs*. Often the interconnects represent regular structures which can be described through mirroring and periodic spatial continuation of a given subspace. In the case of fields which can be described by the Poisson equation the mirroring can be accomplished by applying homogeneous Neumann boundary conditions at the mirroring surface, which can be implemented with the Finite Element Method (FEM) in quite a natural way. However, the periodic boundaries require special treatment for the numerical discretization and grid generation.

Keywords: periodic boundaries, capacitance extraction, electric field calculation.

1 Introduction

Certain elements of integrated circuits like busses or memory cells make use of periodic structures [1, 2]. As example a part of an interconnect bus is shown in Fig. <1>. Often the capacitance between the wires must be extracted which requires the calculation of the electric field, where the wires are connected alternately to 0 V and to 1 V [3]. An appropriately fine resolution of the simulation area is important for the accuracy and leads unfortunately for such domains as in Fig. <1> to the generation of a huge number of nodes. Therefore the simulation process will demand a lot of memory, and the simulation duration can be unacceptably long. Considering the periodicity of the structure of Fig. <1> in direction of the x axis there is a smart way to solve the problem by investigating only one geometrical period of the structure. A possible geometrical period is the area shown in Fig. <2>. The electrodes for the capacitance extraction consist of one interconnect line connected to 1 V and two parts of the neighbor lines connected to 0 V, respectively, which can be seen in the top view in Fig. <3>. The interconnect bus of Fig. <1> can be created by periodic spatial continuation of the area of Fig. <2> along the x axis. Therefore it is not necessary to simulate the whole area of Fig. <1>. It is sufficient to simulate a single cell of periodicity as in Fig. <2>. The simulation has been performed by our software *Smart Analysis Programs* [4]. It is based on the Finite Element Method (FEM) using tetrahedron grids [5, 6, 7]. The algorithm for the linear algebraic equations arising from the finite element discretization is based on the iterative conjugate gradient method which uses an incomplete Cholesky pre-conditioning technique to speed up the iteration convergence [8, 9, 10, 11]. The solution of the Laplace equation in the dielectric is completely extracted from the data defined on the dielectric boundary. Usually the electrodes are represented by Dirichlet boundary conditions and the outer boundary of the

simulation domain by homogeneous Neumann conditions which can be implemented with FEM in a quite natural way. Homogenous Neumann conditions on a planer surface effect the field in the simulation area in such way, as if the simulation area would be mirrored at the respective boundary face. Such "mirroring conditions" can be exploited for the simulation of symmetric structures and periodic structures which exhibit symmetry. However for general periodic structures proper boundary conditions must be implemented which require special treatment.

2 Electric Field Calculation and Capacitance Extraction with Periodic Boundary Conditions

To solve the electric field $\vec{E}$ for the static case the following equations are used:

$$\vec{\nabla} \times \vec{E} = 0 \tag{1}$$

$$\vec{\nabla} \cdot \vec{D} = \rho \tag{2}$$

The solution of (1) is

$$\vec{E} = -\vec{\nabla}\varphi, \tag{3}$$

Inserting (3) in (2) under consideration of the relationship between the electric displacement and electric field ($\vec{D} = \epsilon_0 \underset{\sim}{\epsilon_r} \cdot \vec{E}$) leads to the Poisson equation

$$L[\varphi] = \vec{\nabla} \cdot (\underset{\sim}{\epsilon_r} \cdot \vec{\nabla}\varphi) = -\frac{\rho}{\epsilon_0} \tag{4}$$

The insulators are free of electric charge ($\rho = 0$). Therefore, the solution of (4) is completely determined by the conditions defined on the boundary $\partial\mathcal{V}_D$ (the index D denotes "dielectric"). On the one part of this boundary ($\partial\mathcal{V}_{D1}$) Dirichlet conditions are applied: $\varphi(\vec{r}) = \varphi_0$. On the other part ($\partial\mathcal{V}_{D2}$) Neumann conditions: $D_n\varphi = \vec{n} \cdot (\underset{\sim}{\epsilon_r} \cdot \vec{\nabla}\varphi(\vec{r})) = f_0$. The periodic boundary conditions are defined by two planes ($\mathcal{A}_{p1}$ and $\mathcal{A}_{p2}$) delimiting the simulation area. Each node of the first plane is mapped bidirectionally and uniquely to a corresponding node on the second plane. Although each two corresponding points are separated in the space, due to the periodic condition, they should behave as if they were attached to each other. If $\vec{r}_{p1}$ is the position pointer to a simulation point of $\mathcal{A}_{p1}$ and $\vec{r}_{p2}$ is the position pointer to the corresponding simulation point of $\mathcal{A}_{p2}$ then $\varphi(\vec{r}_{p1}) = \varphi(\vec{r}_{p2})$ for each point of $\mathcal{A}_{p1}$ and $\mathcal{A}_{p2}$.

For the numerical discretization FEM is used with a classical weighted residual approach. Thus, the electric potential φ in $\mathcal{V}_D$ is approximated by:

$$\varphi \approx \tilde{\varphi} = \sum_{j=1}^{n} c_j N_j(\vec{r}) + v(\vec{r}), \text{ where } v = \varphi_0 \text{ on } \partial\mathcal{V}_{D1}, \text{ and } N_j(\vec{r}) = 0 \text{ on } \partial\mathcal{V}_{D1} \text{ for } \forall j. \tag{5}$$

c_j are unknown coefficients and $N_j(\vec{r})$ and $v(\vec{r})$ are known functions. The functions N_j, also called basis functions must build a complete function system. The unknown coefficients c_j are calculated by enforcing the condition

$$\int_{\mathcal{V}_D} W_i R_{\mathcal{V}_D} \mathrm{d}V + \int_{\partial\mathcal{V}_{D2}} \overline{W_i} R_{\partial\mathcal{V}_{D2}} \mathrm{d}A = 0, \quad 1 \le i \le n \tag{6}$$

where the domain residual

$$R_{\mathcal{V}_D} = L[\tilde{\varphi} - \varphi] = L[\tilde{\varphi}] = \vec{\nabla} \cdot (\underset{\sim}{\epsilon_r} \cdot \vec{\nabla}\tilde{\varphi}), \quad \rho = 0 \tag{7}$$

and the boundary residual

$$R_{\partial\mathcal{V}_{D2}} = D_n(\tilde{\varphi} - \varphi) = D_n\tilde{\varphi} - f_0 \tag{8}$$

are multiplied with a set of weighting functions $W_i(\vec{r})$, respectively $\overline{W_i(\vec{r})}$. Inserting (7) and (8) in (6) leads to

$$\int_{\mathcal{V}_D} W_i\vec{\nabla}\cdot(\underset{\sim}{\epsilon_r}\cdot\vec{\nabla}\tilde{\varphi})\mathrm{d}V + \int_{\partial\mathcal{V}_{D2}} \overline{W_i}(D_n\tilde{\varphi} - f_0)\mathrm{d}A = 0 \tag{9}$$

Using the first scalar Green's theorem $\int_{\mathcal{V}_D} W_i\vec{\nabla}\cdot(\underset{\sim}{\epsilon_r}\cdot\vec{\nabla}\tilde{\varphi})\mathrm{d}V = \int_{\partial\mathcal{V}_D} W_i D_n\tilde{\varphi}\mathrm{d}A - \int_{\mathcal{V}_D}\vec{\nabla}W_i\cdot(\underset{\sim}{\epsilon_r}\cdot\vec{\nabla}\tilde{\varphi})\mathrm{d}V$ and choosing $W_i = -\overline{W_i}$ and $W_i = N_i$ (Galerkin method), a linear equation system for the unknown coefficients c_i is obtained

$$\sum_{j=1}^{n} c_j \int_{\mathcal{V}_D}\vec{\nabla}N_i\cdot(\underset{\sim}{\epsilon_r}\cdot\vec{\nabla}N_j)\mathrm{d}V = \int_{\partial\mathcal{V}_{D2}} N_i f_0\mathrm{d}A - \int_{\mathcal{V}_D}\vec{\nabla}N_i\cdot(\underset{\sim}{\epsilon_r}\cdot\vec{\nabla}v)\mathrm{d}V,\ 1\le i\le n. \tag{10}$$

Homogeneous or mirroring boundary conditions mean $f_0 = 0$. Therefore homogeneous Neumann conditions can be implemented simply by omitting the boundary integral term from (10). This means that every part of the boundary, where no special conditions are enforced implicitly has homogeneous Neumann conditions.

The simulation domain $\mathcal{V}_D$ is discretized in tetrahedral elements. To each node $\vec{r_j}$ of $\mathcal{V}_D$ basis function N_j is assigned, which has the value of 1 in the node j and 0 in all other nodes. Each function N_j is different from 0 only in the elements, which are directly attached to the node j, and vanishes in all other elements. If due to the discretization N points are created in $\mathcal{V}_D$, the points which do not belong to $\partial\mathcal{V}_{D1}$ are numbered by $1\le j\le NU$ and the nodes at $\partial\mathcal{V}_{D1}$ are numbered by $NU+1\le j\le N$. Then the function v can be expressed as $v = \sum_{j=NU+1}^{N} c_j N_j$ in $\partial\mathcal{V}_{D1}$ with known N_j and c_j ($c_j = \varphi_0(\vec{r_j})$, $\vec{r_j}$ on $\partial\mathcal{V}_{D1}$). Therefore (10) leads to

$$\sum_{j=1}^{NU} c_j \int_{\mathcal{V}_D}\vec{\nabla}N_i\cdot(\underset{\sim}{\epsilon_r}\cdot\vec{\nabla}N_j)\mathrm{d}V = -\sum_{j=NU+1}^{N} c_j \int_{\mathcal{V}_D}\vec{\nabla}N_i\cdot(\underset{\sim}{\epsilon_r}\cdot\vec{\nabla}N_j)\mathrm{d}V,\quad 1\le i\le NU \tag{11}$$

Naturally the points produced by the grid generation software are not ordered as in (11). To obtain the desired node ordering an additional index array with length N is allocated. The first NU entries of this index array refer to the nodes in $\mathcal{V}_D$ without $\partial\mathcal{V}_{D1}$. The remaining entries (from NU till N) refer to the nodes on the Dirichlet boundary $\partial\mathcal{V}_{D1}$. The additional index assignment of the simulation nodes gives advantages to the implementation of the periodic boundary conditions. Each two corresponding points of the plains $\mathcal{A}_{p1}$ and $\mathcal{A}_{p2}$ get the same index in the additional index array. Thus, they are assembled in the system linear equation (11) as if they were the same point. The periodic condition also requires that each periodic point must be connected not only to his neighbor nodes but also to the neighbor nodes of the corresponding periodic point, which is automatically fulfilled by the element-by-element assembling of the linear equation system (11).

The numerical capacitance calculation uses commonly the energy method $C = U^2/(2W)$, where U is the voltage applied between the conductors and W is the electric energy stored in the dielectric $\mathcal{V}_D$.

$$W = \int_{\mathcal{V}_D}\vec{E}\cdot\vec{D}\mathrm{d}V = \epsilon_0\int_{\mathcal{V}_D}\vec{E}\cdot(\underset{\sim}{\epsilon_r}\cdot\vec{E})\mathrm{d}V.$$

Thus, C is calculated from the electric field $\vec{E}$, given by (3).

3 Grid Generation

Although periodic boundary conditions can be applied to an arbitrary pair of faces with unique bidirectional node mapping we will restrict this paragraph to parallelepiped structures for the sake of clarity. The periodic boundary conditions are applied at two opposite parallel faces. The grid generated has to guarantee that the surface grids on these faces are identical. Our interconnect simulation software *Smart Analysis Programs* uses two different three-dimensional grid generation approaches. The first one is a layered approach which extends two-dimensional grid generator [12] into the third dimension by means of linear extrusion. The second approach is a fully unstructured grid generation method based on the program delink [13, 14]. Both approaches do not fulfill the above mentioned requirements for periodic boundaries a priori. To extend the grid generator for periodic boundaries we use an iterative approach. In the first step the simulation domain is meshed without any special treatment for periodic boundaries. Afterwards the periodic boundary faces are checked for conformity. If they are not conform they are merged and the newly generated points are fed into the grid generator as additional input. After re-meshing of the geometry the periodic boundaries are again checked for conformity. These steps are repeated until conformity is reached. In the layer based meshing approach this iteration procedure must only be applied to the two-dimensional grid generation process. The additional extrusion step preserves the conformity of the side walls. In the fully unstructured meshing method the conformity of the nodes on the periodic faces is not sufficient, because the same set of boundary nodes can lead to different boundary meshes (at least for cospherical points). Therefore also edge conformity has to be guaranteed during the iteration. Because of these additional difficulties the layer based grid generation method is preferred for problems with periodic boundaries. Unfortunately, we were not able to prove theoretically that the iteration process necessary for fully unstructured grids will always terminate, however we have not found any example so far, which took more than 11 iterations.

4 Simulation Results

The simulation results are evaluated by visualization of the electric field using VTK [15, 16]. In the presented example the simulation area consists of a SiO2 rectangular parallelepiped with the conductors inside as shown in Fig. <2>. The faces parallel to the yz plane are defined as periodic boundary. At the remaining outer faces homogeneous Neumann boundary conditions are applied. The simulated potential and the corresponding iso faces with periodic boundary conditions are shown in Fig. <4> and Fig. <5>. The electric field is equivalent to the electric field in an inner single cell of the original interconnect bus structure. That is as if the simulation domain would be copied repeatedly in x and -x direction by the length of its x dimension. The electric field looks like as if one boundary parallel to yz plane would be directly connected to the opposite one. The stamp of the electrodes which are lying on the one of the periodic faces can be seen on the other periodic face. In order to visualize the effect of the periodic boundary conditions, the same structure has been simulated with homogeneous Neumann boundaries (natural boundary conditions) for comparison. The obtained electric potential distribution is displayed in Fig. <6> and Fig. <7>. In this case the effect of the opposite electrodes is no longer seen on the side walls and the iso surfaces are now perpendicular to the boundary. The field in the simulation area is as if the simulation area would be mirrored with respect to these boundaries. As expected the calculated capacitance between the electrodes in the small area from Fig. <2> is different for the different boundary conditions applied. The capacitance with the periodic boundary is 1.33 times the capacitance with homogeneous Neumann boundary. The capacitance of the whole area from Fig. <1> is the capacitance of the small simulation domain multiplied by the number of all small simulation domains needed to construct the complete structure.

References

[1] N. Thepayasuwan, A. Doboli, "Layout Conscious Bus Architecture Synthesis for Deep Submicron Systems on Chip in Design", Automation and Test in Europe Conference and Exhibition, 1530-1591/04, 2004 IEEE

[2] I. Koren, Z. Koren, and D. Pradhan, "Designing Interconnection Buses in VLSI and WSI for Maximum Yield and Minimum Delay", IEEE Journal of Solid State Circuits, vol.23, no. 3, June 1988.

[3] R. Sabelka, C. Harlander, S. Selberherr, "The State of the Art in Interconnect Simulation", International Conference on Simulation of Semiconductor Processes and Devices, 2000, 6–11.

[4] R. Sabelka and S. Selberherr, "A Finite Element Simulator for Three-Dimensional Analysis of Interconnect Structures", Microelectronics Journal, vol. 32, pp. 163 171, Jan. 2001.

[5] J.L. Volakis, A. Chatterjee, L.C. Kempel, *Finite Element Method for Electromagnetics*, IEEE Press, New York, ISBN 0-7803-3425-6, 1998.

[6] T.R. Chandrupatla, A.D.Belegundu, *Introduction to Finite Elements in Engineering*, Third Edition, ISBN 0-13-178453-6

[7] R. Sabelka, "Dreidimensionale Finite Elemente Simulation von Verdrahtungsstrukturen auf Integrierten Schaltungen", Dissertation, Technische Universität Wien, 2001, http://www.iue.tuwien.ac.at/phd/sabelka.

[8] R. Bauer and S. Selberherr, "Preconditioned CG-Solvers and Finite Element Grids", in Proc. CCIM, vol. 2, (Breckenridge, USA), Apr. 1994.

[9] J. R. Shewchuk, "An Introduction to the Conjugate Gradient Method without the Agonizing Pain", http://www2.cs.cmu.edu/˜jrs/jrspapers.html, Aug. 1994.

[10] S. C. Eisenstat, "Efficient Implementation of a Class of Preconditioned Conjugate Gradient Methods", SIAM J.Sci.Stat.Comput., vol. 2, no. 1, pp. 1–4, 1981.

[11] T. A. Manteuffel, "The Shifted Incomplete Cholesky Factorization", in Sparse Matrix Proceedings, I.S. Duff and G.W. Stewart, Eds., 1979, pp. 41–61.

[12] J. R. Shewchuk, "Triangle: Engineering a 2D Quality Mesh Generator and Delaunay Triangulator", in Proc. First Workshop on Applied Computational Geometry. May 1996, pp. 124-133, Association for Computing Machinery.

[13] P. Fleischmann, R. Sabelka, A. Stach, R. Strasser, and S. Selberherr, "Grid Generation for Three-dimensional Process and Device Simulation", In SISPAD'96 [37], pp. 161–166.

[14] P. Fleischmann and S. Selberherr, "A New Approach to Fully Unstructured Three-dimensional Delaunay Mesh Generation with Improved Element Quality", In SISPAD'96 [37], pp. 129–130.

[15] W. Schroeder, K. Martin, and B. Lorensen, *The Visualization Toolkit: An Object-Oriented Approach to 3D Graphics*, Prentice-Hall, 1996.

[16] W. Schroeder, K. Martin, and B. Lorensen, "The Visualization Toolkit (VTK) Home Page", http://www.kitware.com/vtk.html.

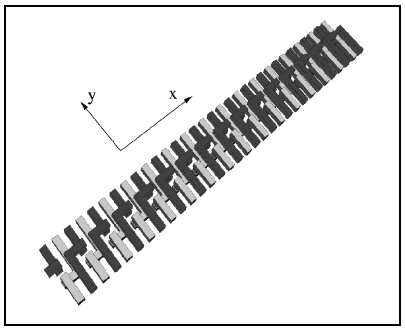

Figure 1: *An interconnect bus.*

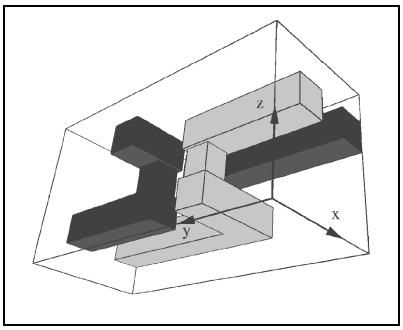

Figure 2: *The simulation area.*

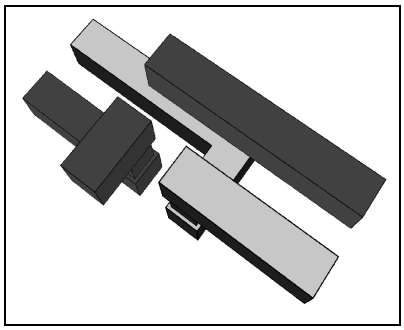

Figure 3: *The electrodes in the simulation area.*

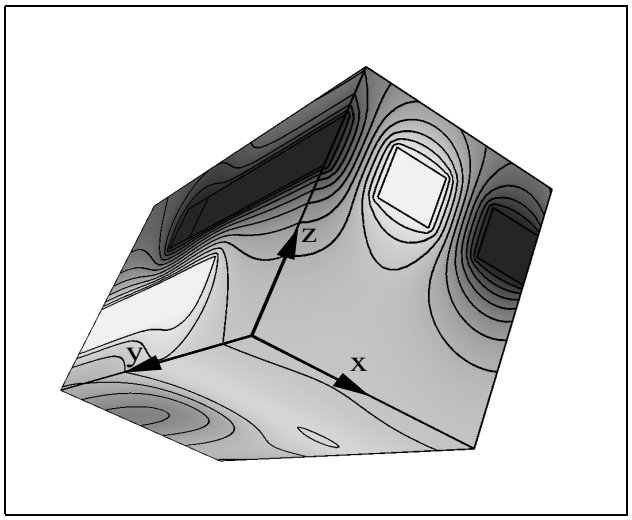

Figure 4: *The electric potential distribution with x periodicity.*

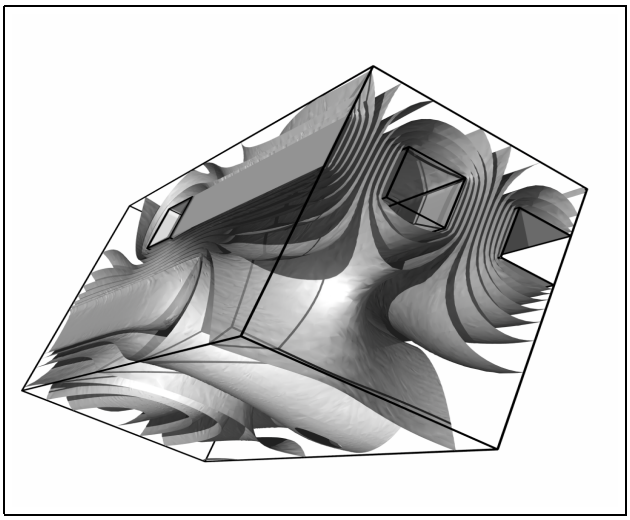

Figure 5: *The iso faces of the electric potential distribution with x periodicity.*

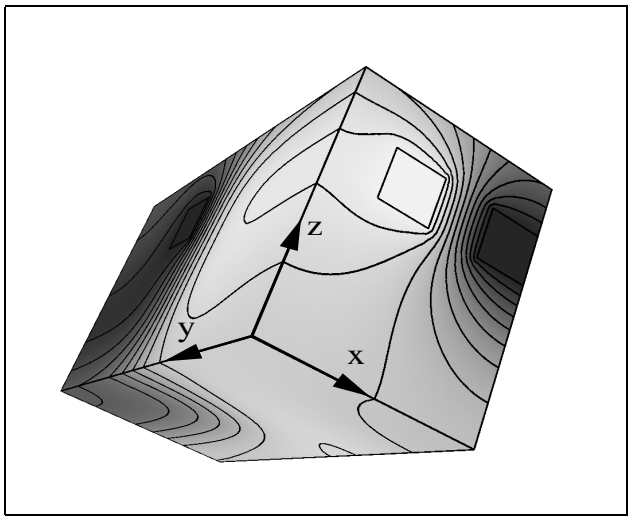

Figure 6: *The electric potential distribution without periodicity.*

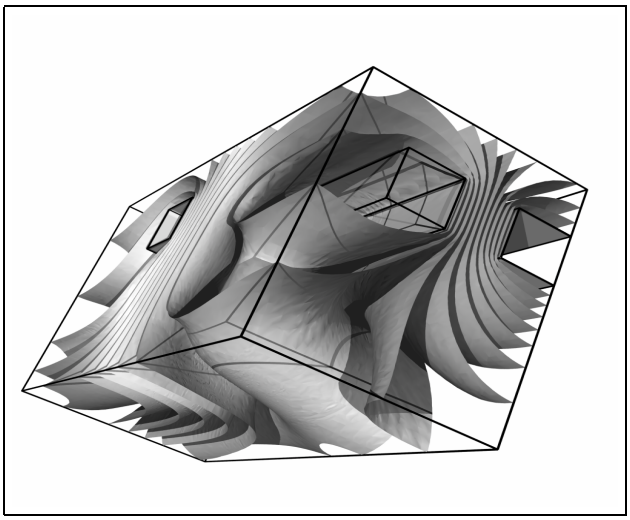

Figure 7: *The iso faces of the electric potential distribution without periodicity.*